Supporting information

Direct modulation of localized surface plasmon coupling of gold nanoparticles on solid substrates via weak polyelectrolyte mediated layer-by-layer self assembly

Contents: 1. UV-visible spectra of the nanocomposite films with different bilayer number assembled at different pH and the evolution of the intensity ratio of transverse band peak adsorption to longitudinal band peak adsorption with bilayer number at different assembly pH (Figure S1, Figure S2, Figure S3, Figure S4).

2. UV-visible spectra fitting of pH 3.4 film using Gaussian distribution function (Figure S5).

3. UV-visible spectra of the nanocomposite films (after baseline correction) assembled at different pH after immersed in different environment for one month (pH 10.0 alkaline solution, pH 3.5 alkaline solution, and 10mM PBS) (Figure S6-Figure S14).

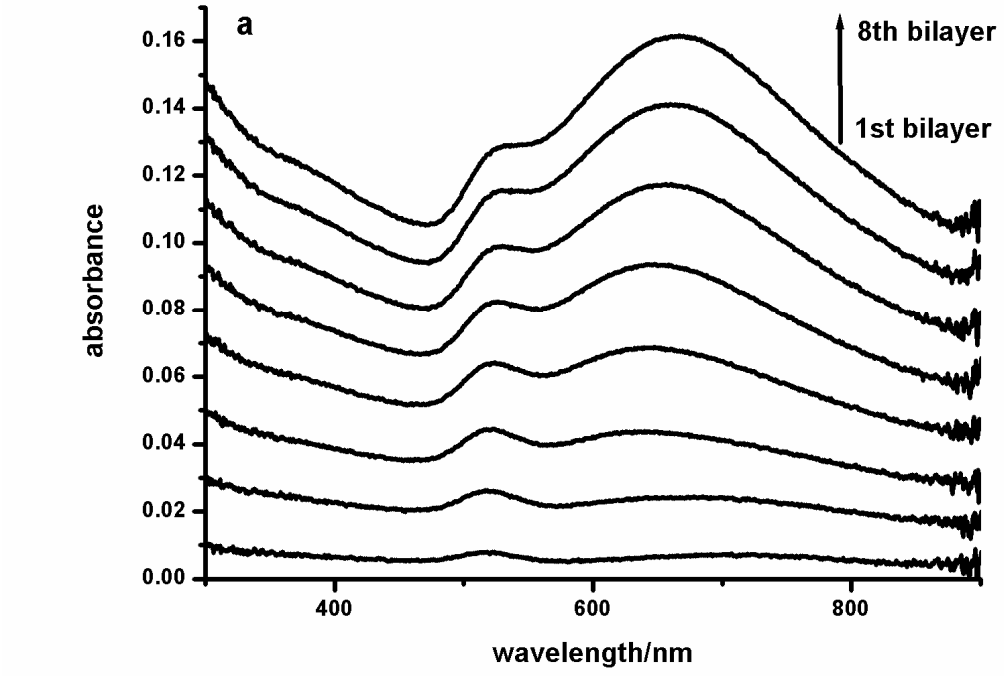

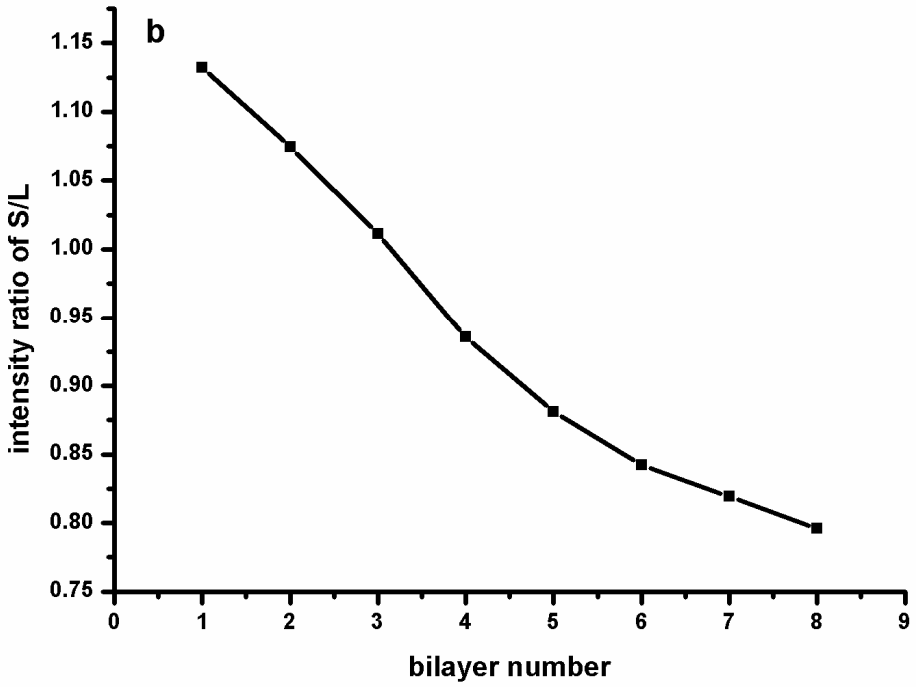


Figure S1. UV-visible spectra of the nanocomposite assembled at pH 5.6 (a) and the intensity ratio of transverse band peak adsorption to longitudinal band peak adsorption versus the bilayer number of the nanocomposite films assembled at pH 5.6 (b).

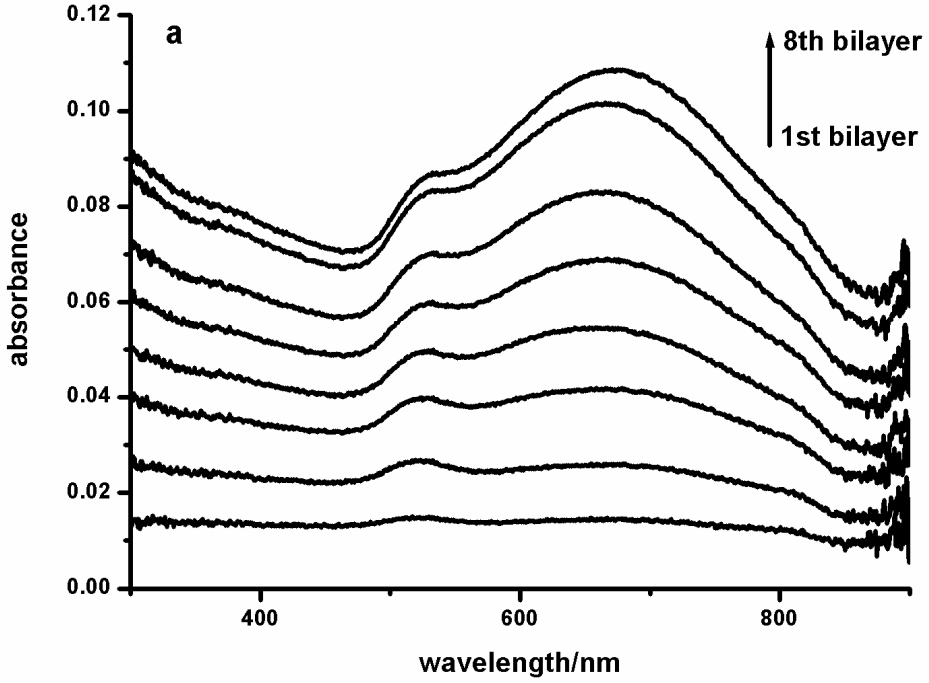
a
8th bilayer
1st bilayer
absorbance
0.12
0.10
0.08
0.06
0.04
0.02
0.00
400
600
800
wavelength/nm

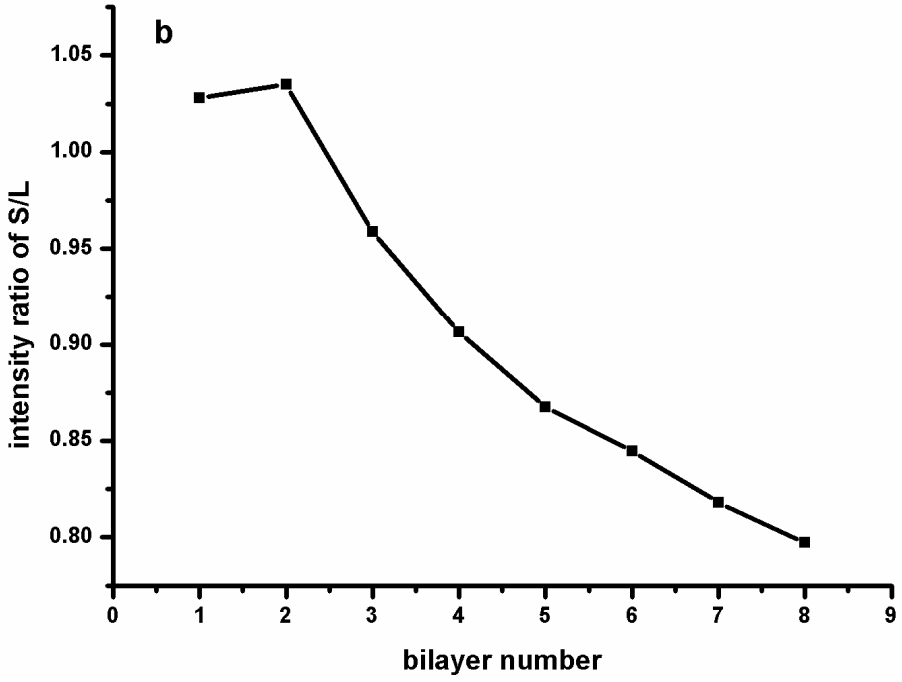
b
intensity ratio of S/L
1.05
1.00
0.95
0.90
0.85
0.80
0
1
2
3
4
5
6
7
8
9
bilayer number

Figure S2. UV-visible spectra of the nanocomposite assembled at pH 6.8 (a) and the intensity ratio of transverse band peak adsorption to longitudinal band peak adsorption versus the bilayer number of the nanocomposite films assembled at pH 6.8 (b).

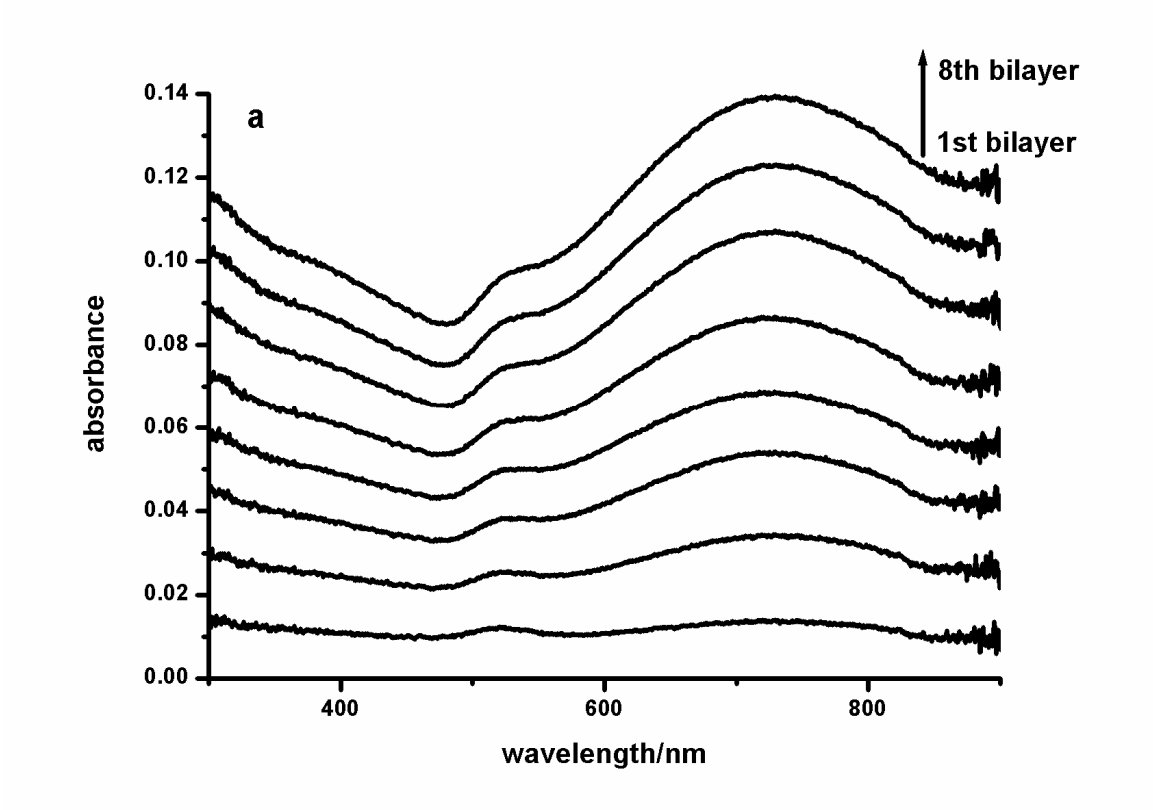

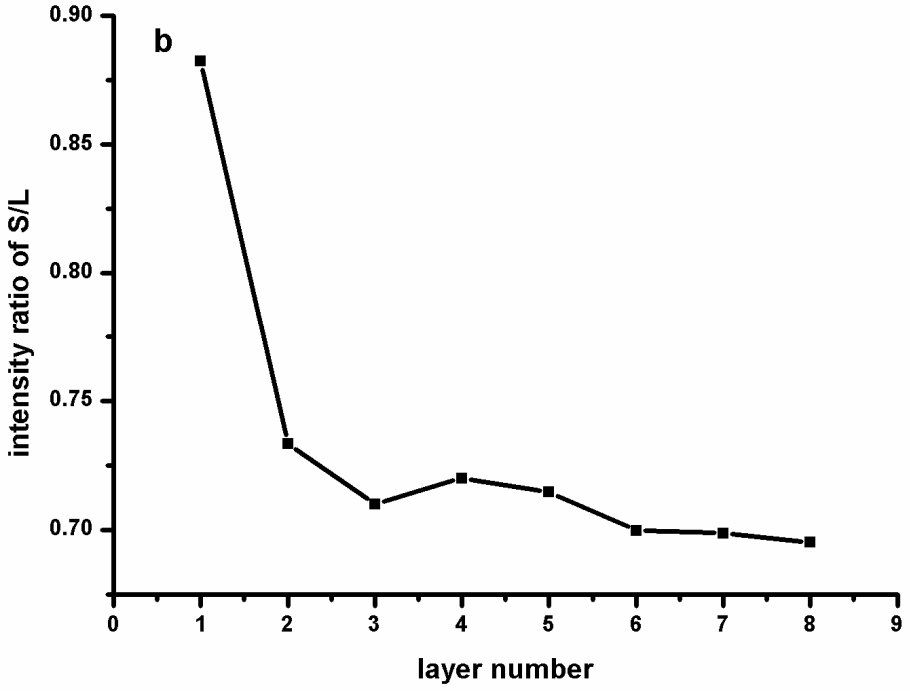


Figure S3. UV-visible spectra of the nanocomposite assembled at pH 7.2 (a) and the intensity ratio of transverse band peak adsorption to longitudinal band peak adsorption versus the bilayer number of the nanocomposite films assembled at pH 7.2 (b).

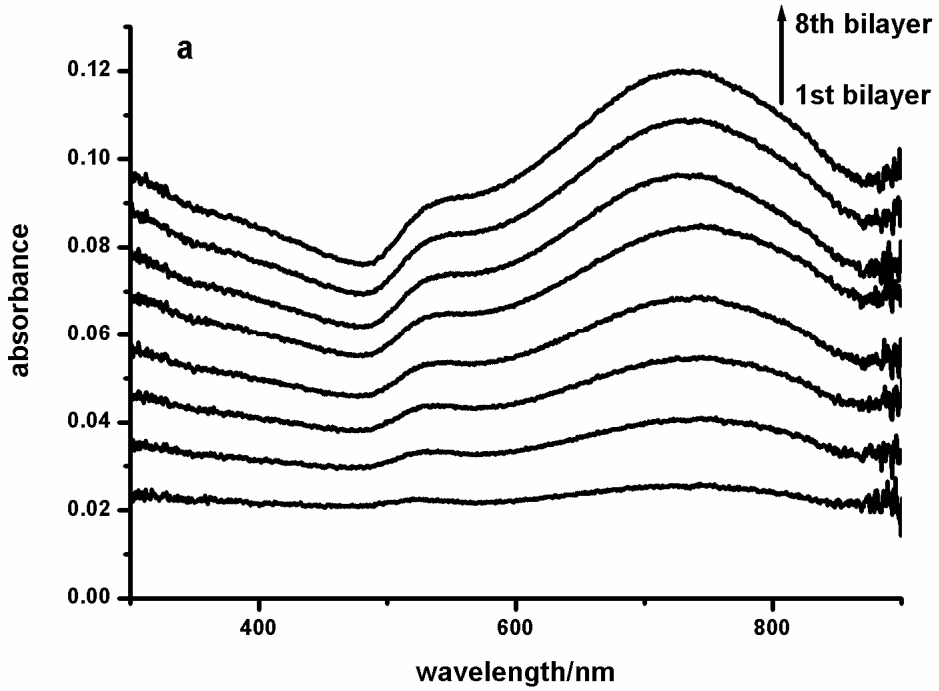
a
8th bilayer
1st bilayer
absorbance
0.12
0.10
0.08
0.06
0.04
0.02
0.00
400
600
800
wavelength/nm

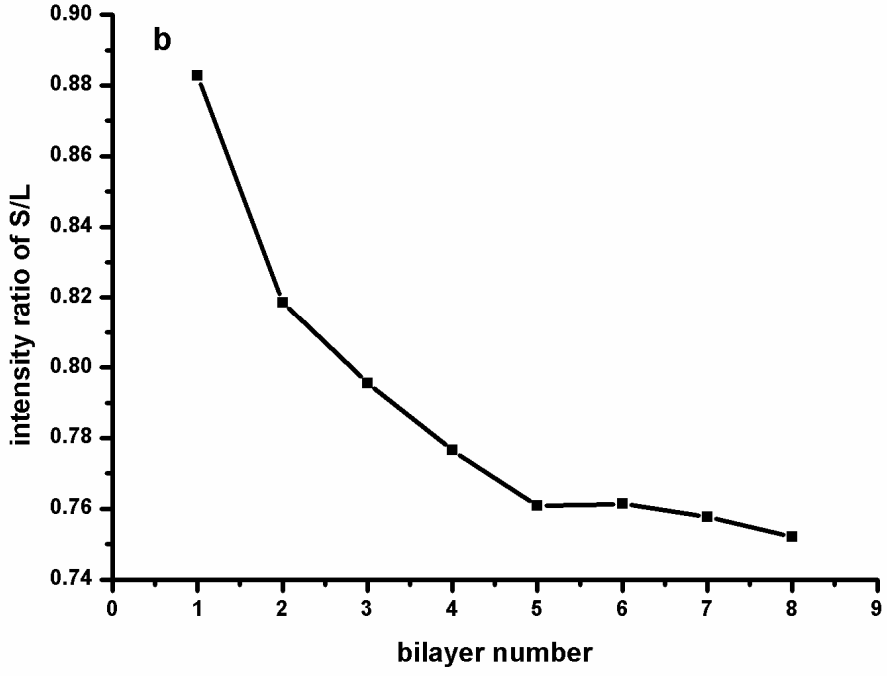
b
intensity ratio of S/L
0.90
0.88
0.86
0.84
0.82
0.80
0.78
0.76
0.74
0
1
2
3
4
5
6
7
8
9
bilayer number

Figure S4. UV-visible spectra of the nanocomposite assembled at pH 10.0 (a) and the intensity ratio of transverse band peak adsorption to longitudinal band peak adsorption versus the bilayer number of the nanocomposite films assembled at pH 10.0 (b).

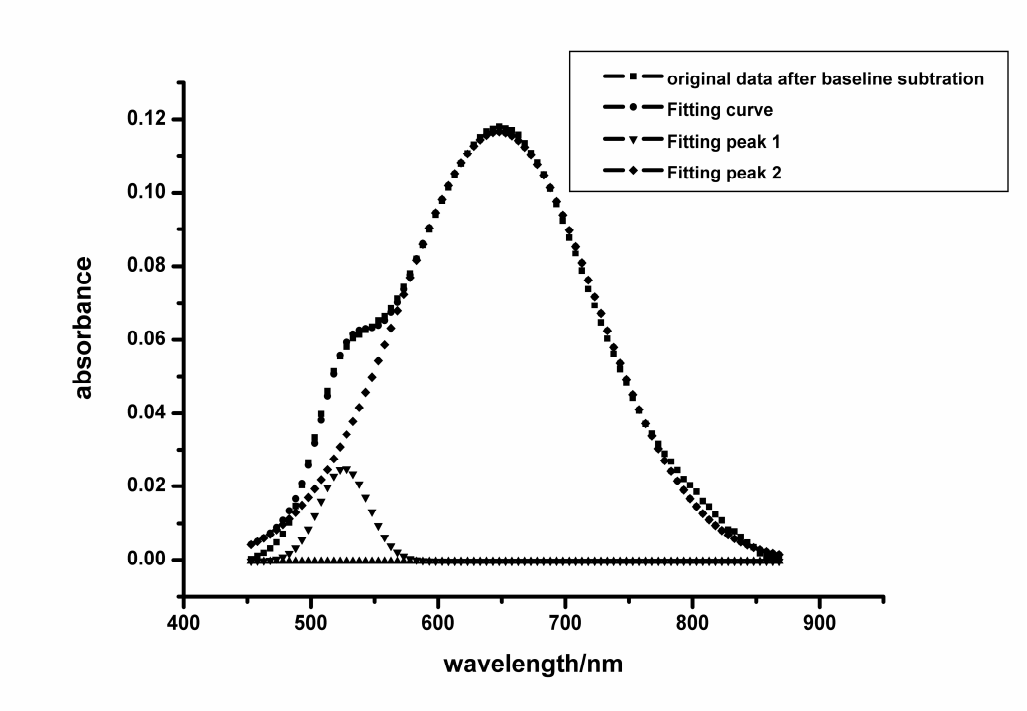


Figure S5. UV-visible spectra fitting of pH 3.4 film using Gaussian distribution function.

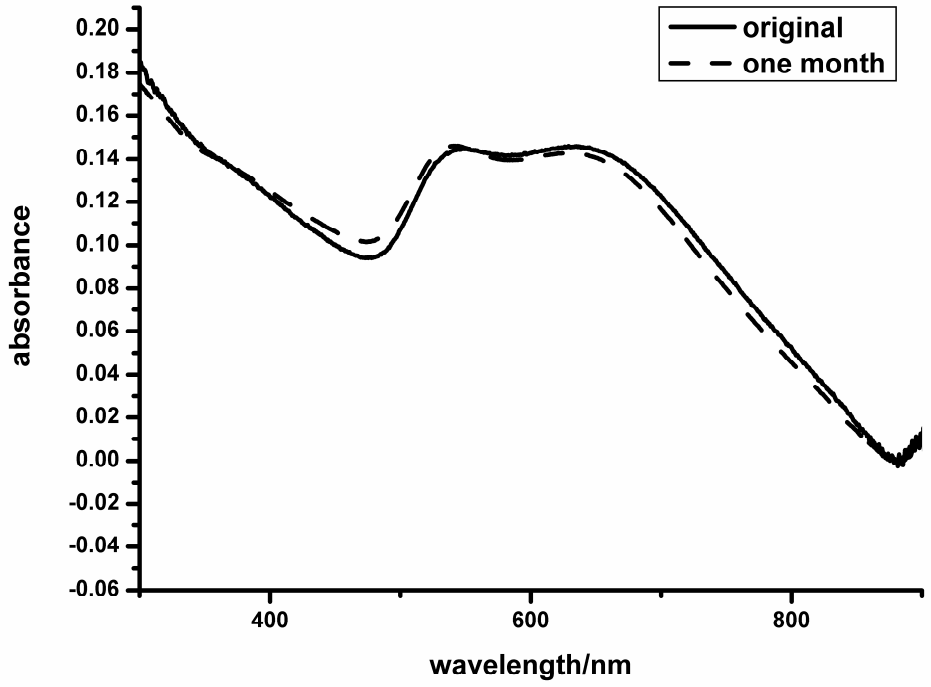


Figure S6. UV-visible spectra of the nanocomposite films assembled at pH 3.4 before and after one month immersion in pH 10 alkaline solution.

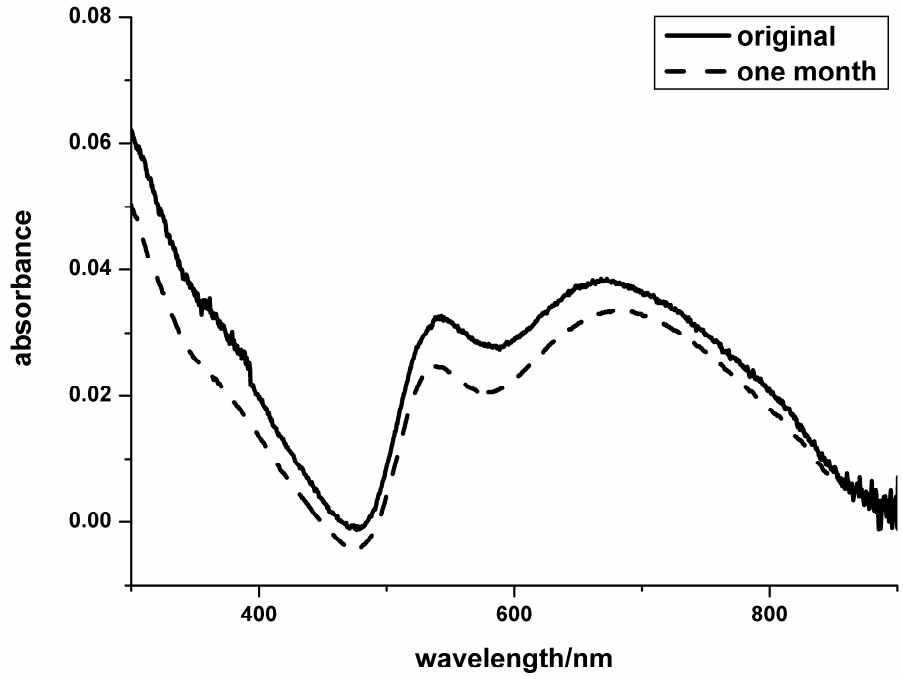

Figure S7. UV-visible spectra of the nanocomposite films assembled at pH 5.6 before and after one month immersion in pH 10 alkaline solution.

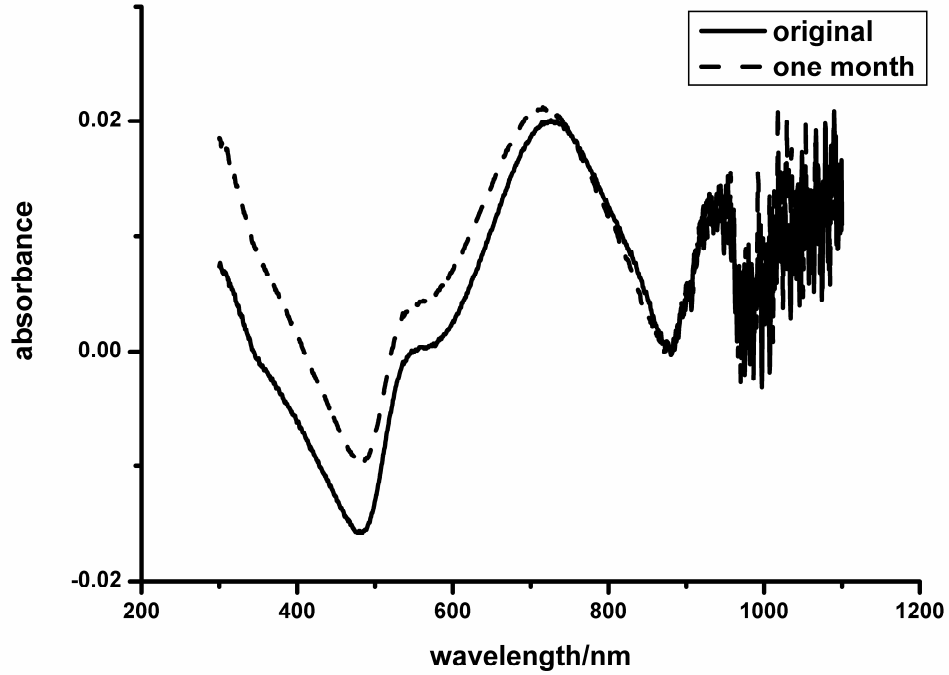


Figure S8. UV-visible spectra of the nanocomposite films assembled at pH 10.0 before and after one month immersion in pH 10 alkaline solution.

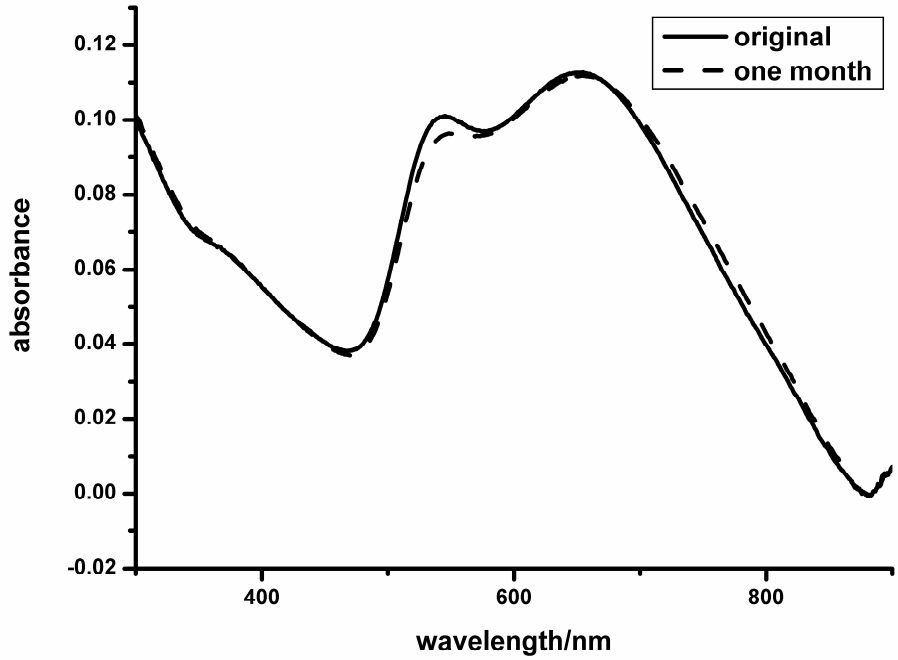

Figure S9. UV-visible spectra of the nanocomposite films assembled at pH 3.4 before and after one month immersion in pH 3.5 acidic solution.

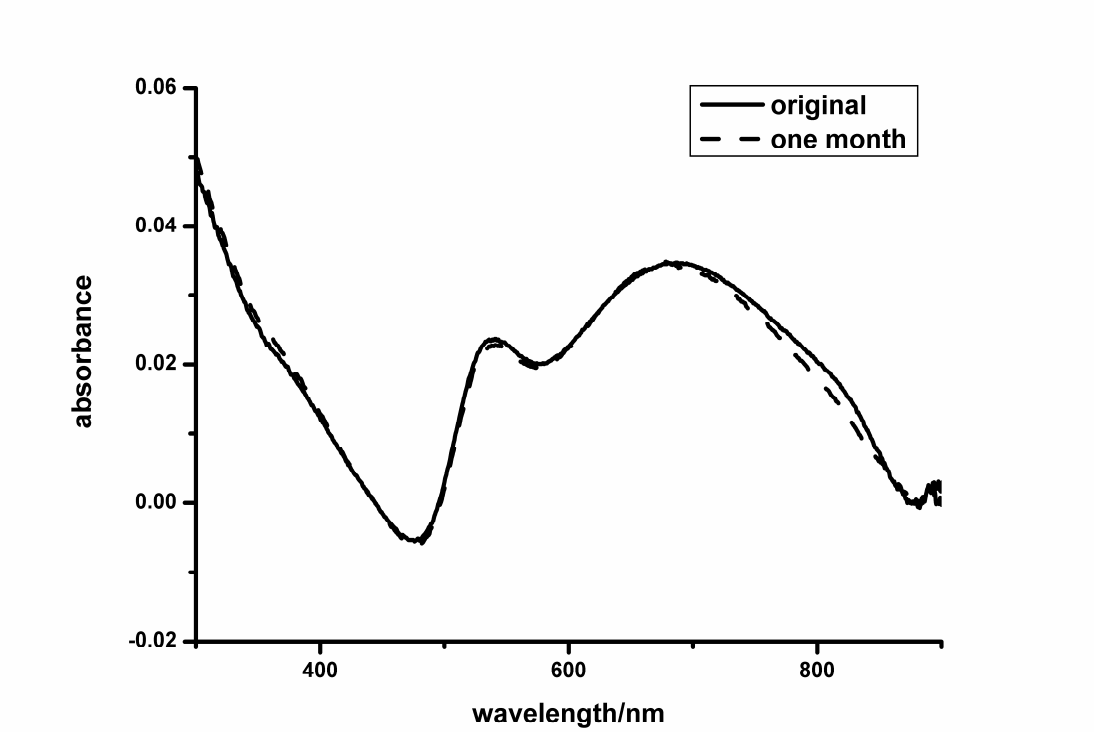


Figure S10. UV-visible spectra of the nanocomposite films assembled at pH 5.6 before and after one month immersion in pH 3.5 acidic solution.

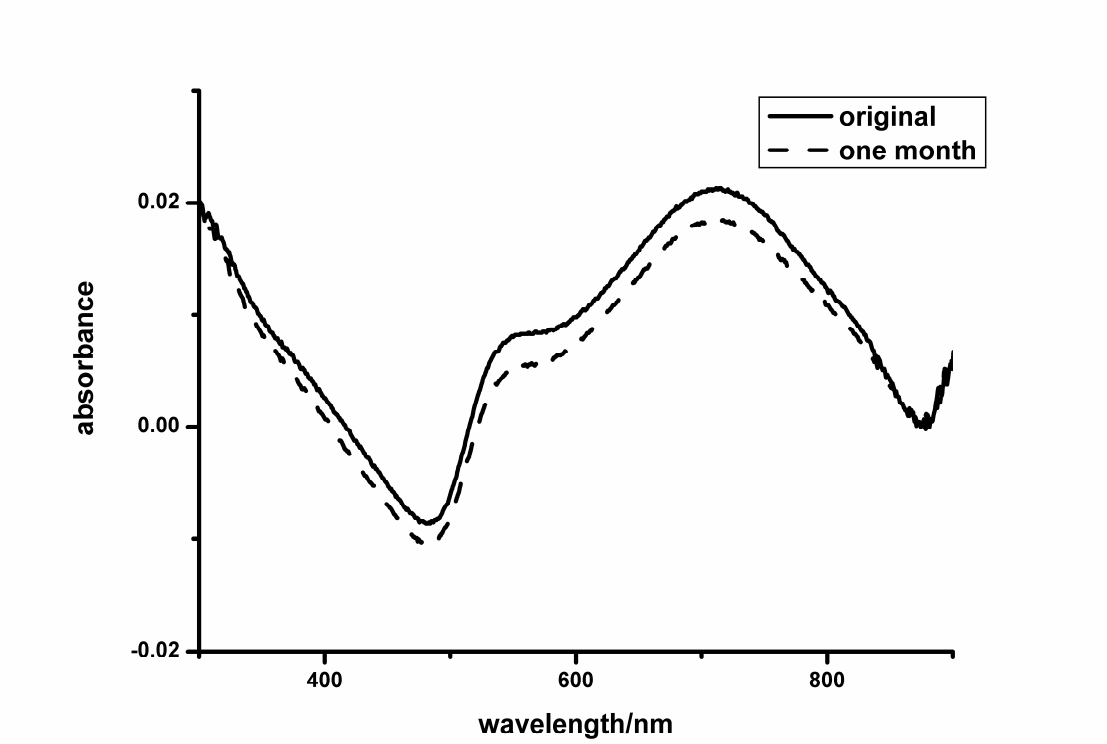


Figure S11. UV-visible spectra of the nanocomposite films assembled at pH 10.0 before and after one month immersion in pH 3.5 acidic solution.

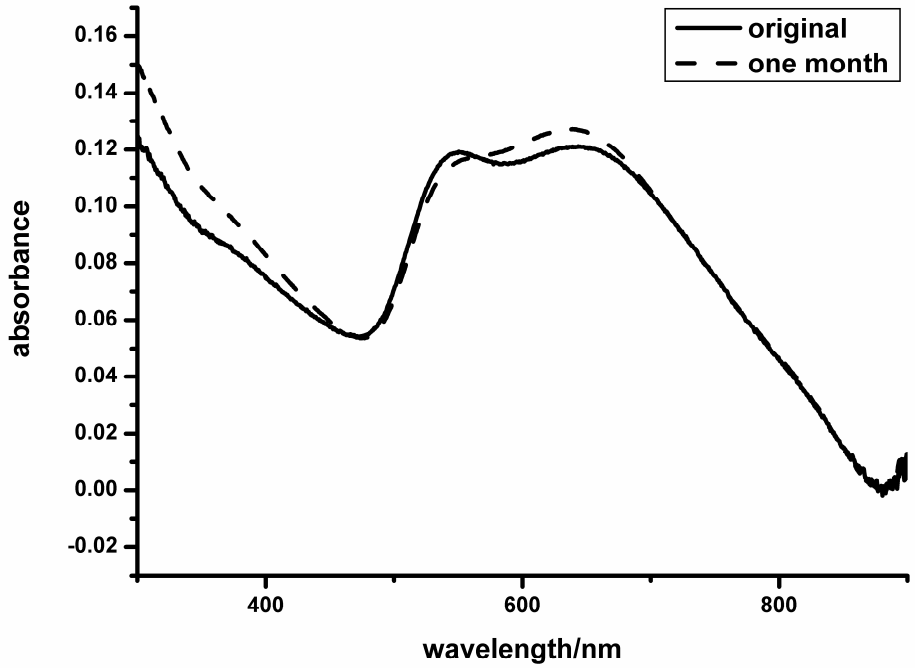


Figure S12. UV-visible spectra of the nanocomposite films assembled at pH 3.4 before and after one month immersion in 10mM PBS.

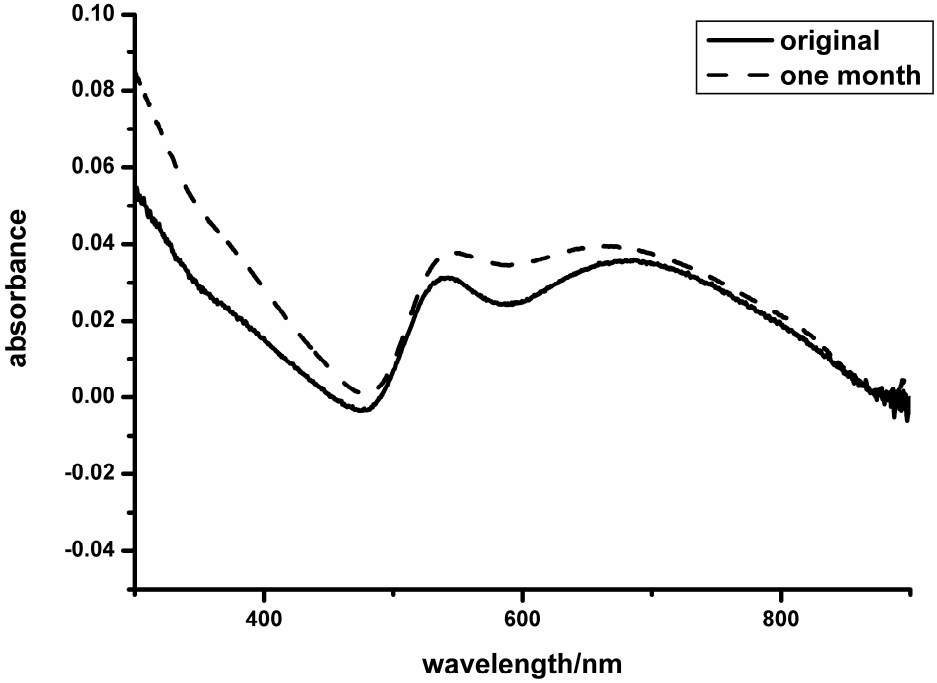

Figure S13. UV-visible spectra of the nanocomposite films assembled at pH 5.6 before and after one month immersion in 10mM PBS.

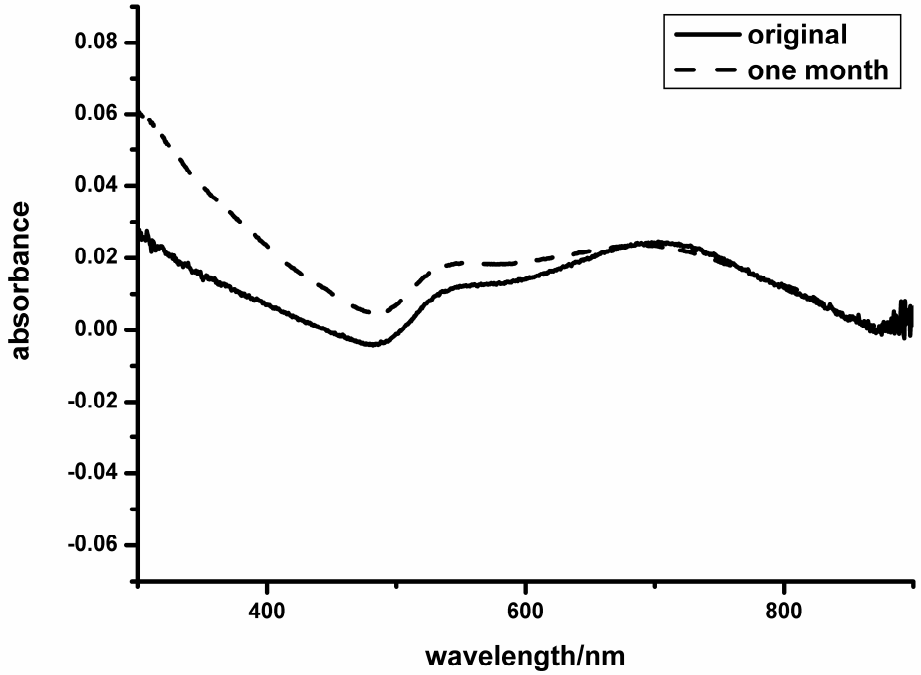


Figure S14. UV-visible spectra of the nanocomposite films assembled at pH 10.0 before and after one month immersion in 10mM PBS.